International Journal of Mass Spectrometry 305 (2011) 20–25

Contents lists available at ScienceDirect

International Journal of Mass Spectrometry

journal homepage: www.elsevier.com/locate/ijms

Vacuum ultraviolet negative photoion spectroscopy of dichlorodifluoromethane

Liu-Li Chen[a], Shan Xi Tian[a,*], Yun-Feng Xu[a], Gen-Bai Chu[b], Fu-Yi Liu[b], Xiao-Bin Shan[b], Liu-Si Sheng[b]

[a] Hefei National Laboratory for Physical Sciences at the Microscale and Department of Chemical Physics, University of Science and Technology of China, Hefei, Anhui 230026, China
[b] National Synchrotron Radiation Laboratory, University of Science and Technology of China, Hefei, Anhui 230029, China

ARTICLE INFO

Article history:
Received 21 January 2011
Received in revised form 19 April 2011
Accepted 19 April 2011
Available online 28 April 2011

Keywords:
Ion-pair photodissociation
Dichlorodifluoromethane
Rydberg states
Thermochemistry

ABSTRACT

Negative ions $^{35}Cl^-$, $^{37}Cl^-$, and F^- are observed in the vacuum ultraviolet photodissociations of dichlorodifluoromethane (CF_2Cl_2) using synchrotron radiation and their ion production efficiency curves are recorded in the photon energy range of 8.00—20.50 eV. Two similar spectra of the isotope anions $^{35}Cl^-$ and $^{37}Cl^-$show that besides the strong bands related to the electron transitions from valence to Rydberg states converged to vertical ionization states, there are some additional peaks that can be assigned as the energetically accessible multi-body fragmentation processes, on the basis of the high-level G3MP2 calculations performed in this work and the thermochemistry data available in the literatures. The appearance energy of Cl^- is experimentally determined to be 8.20 ± 0.04 eV, in excellent agreement with the theoretical thermochemical value 8.19 eV. A novel competition between the ion-pair photodissociations to Cl^- and F^- anions is found in the photon energy range of 17.30–20.50 eV.

1. Introduction

As a novel decaying process of the valence electron excitation of a molecule, positive ion–negative ion pair dissociation has been investigated in a broad photon energy range (from vacuum ultraviolet to near X-ray) and for the various molecules [1–8]. Halogen-containing molecules receive much attention, basically owing to two points: the halogen atomic anions are frequently observed in the ion-pair photodissociations because of the high electron affinities (EAs) of the halogen atoms; the photoion-pair formation can occur even below the molecular adiabatic ionization potential (IP_a), such study is accessible using laser systems in laboratory [2]. However, the applications of laser systems are limited, due to the narrow range of tunable photon energies. There are a variety of excited states coupling with the ion-pair states, in particular, for polyatomic molecules, at the photon energies above IP_a values. Synchrotron radiation as the vacuum ultraviolet (VUV) photon source which is tunable in a large scale of energy, together with the time-of-flight (TOF) mass spectrometer, is a unique tool applicable in the ion-pair dissociation studies. A straightforward strategy is to detect the negative ions produced in the ion-pair dissociations with negative mass spectrometer and by scanning photon energies, which is named as ion-pair anion efficiency spectroscopy [4,5,8]. The merit of ion-pair anion efficiency spectra (IPAES) at the photon energies below IP_a is that the ion-pair dissociations shown in the spectra have no interference from the contributions of the photoelectron dissociative attachments. It is noted that at the photon energies above IP_a, the low-energy photoelectron attachments to the target molecules can lead to the molecular dissociations to anionic fragments [9] that are possibly detected with the negative ion TOF mass spectrometer used in the IPAES study. To eliminate the interference from the photoelectron dissociative attachments, the pressure of the photon-molecule reaction area in chamber should be low enough to avoid the secondary reactions between the photoelectron and the target molecule [6,8]. The IPAES exhibit the signal integral of a specific anion produced at a certain photon energy and the less, thus they are similar to the positive photoion efficiency (PIE) spectra in principle [4,5,8,10,11]. Some fine spectral structures observed in the IPAES can be attributed to the resonant transitions or couplings between the ion-pair states and the electron excited states. Interpretations to the IPAES heavily rely on the evidences provided with the other spectroscopic methods, in particular, with the references of the PIE spectra and the high-resolution photoabsorption spectra.

In this work, an experimental study of ion-pair dissociations of dichlorodifluoromethane (CF_2Cl_2) is reported. CF_2Cl_2, known as Freon 12, is responsible for destroying ozone layer in the stratosphere [12]. Its molecular electronic structure has been the subject in many experimental and theoretical studies. The VUV photoabsorption spectra of CF_2Cl_2 were firstly recorded by Zobel and Duncan [13], reexamined by Doucet et al. [14] and Ibuki et al. [15], and recently by Seccombe et al. [16] and Limão Vieira et al. [17]. Threshold photoelectron photoion coincidence spectrum of CF_2Cl_2 was recorded in the photon energy range of 10–25 eV using synchrotron radiation [18]. However, as for the photoelectron spectra,

* Corresponding author. Fax: +86 551 3607084.
E-mail address: sxtian@ustc.edu.cn (S.X. Tian).

1387-3806/$ – see front matter © 2011 Elsevier B.V. All rights reserved.
doi:10.1016/j.ijms.2011.04.004

there are long-term arguments on the spectral assignments, i.e., the spectral terms of the ionization states and their energetic sequence [14–20]. Recently, Shan et al. [21] provided an unambiguous ordering of the ionization states for the outer valence orbitals of CF_2Cl_2 with the high resolution electron momentum spectroscopy technique. To the best of our knowledge, only was the Cl^- production efficiency spectrum of CF_2Cl_2 reported in a narrow energy range of 10.4–11.8 eV [7], while little information is available for the F^- product [22]. Here the fragment yields of Cl^- by the VUV photoexcitation of CF_2Cl_2 have been recorded as a function of photon energy in the range of 8.00–20.50 eV using synchrotron radiation, and the production competition between F^- and Cl^- is observed for the first time in the higher energy range of 17.30–20.50 eV.

2. Experimental methods and thermochemistry calculations

The production efficiency spectra of Cl^- and F^- were measured at the atomic and molecular physics end-station of national synchrotron radiation facility at Hefei, China. The apparatus used in the present ion-pair photodissociation study was described previously in detail [8,23,24]. Briefly, the VUV photon beam was monochromatized with the undulator-based spherical-gratings (made by Horiba Jobin Yvon in France) then focused onto the reaction region. A diffuse molecular beam was introduced with a stainless steel tube (its diameter: 0.5 mm). The anionic fragments were collected with a home-made reflectron TOF mass spectrometer which was installed perpendicularly to the plane containing the molecular beam and the photon beam. Packets of anions were pushed periodically from the reaction region by a pulsed repeller (−165 V voltage, 1.5—2.0 μs pulse width, and 18,000 Hz repetition) into an acceleration region. The pulsed anions were focused and transferred through the drift area, then reflected by the retarding lenses. At last the anions were detected with two zigzag stacking microchannel plates. The wavelength of VUV beam was calibrated and the energy resolution was determined ($E/\Delta E = 5000$) before the present experiments. The energy scanning step and the signal accumulation time at each step were typically 0.02 eV with 60 s at the lower photon energies, and 0.005 eV with 40 s at the higher photon energies, respectively. To normalize the anion signals, the photon flux was monitored with a silicon photodiode (SXUV-100, International Radiation Detectors, Inc.). The commercial sample CF_2Cl_2 (purity > 99.9%) was used after several freeze-pump-thawed cycles.

To access the ion-pair dissociation channel, for example, the diatomic molecule AB: $AB + h\nu \rightarrow A^+ + B^-$, its energetic threshold $E_{\text{ion-pair}}$ is determined by,

$$E_{\text{Threshold}}(B^-) = D_0(AB^+) + IP_a(AB) - EA(B) \quad (1)$$

where $D_0(AB^+)$ is the dissociation energy of AB^+ (to $A^+ + B$), $IP_a(AB)$ is the molecular ionization threshold, i.e., IP_a, and EA(B) is the EA value of atomic B. When $EA(B) > D_0(AB^+)$, the B^- anion can be produced below the ionization threshold, i.e., IP_a.

Since the room-temperature diffuse beam was employed in the present experiments, to evaluate the threshold for an ion-pair dissociation with Eq. (1), we need consider the thermal or internal energy of the parent molecule (at 298 K) while the fragments at 0 K. In the calculations of the ion-pair dissociation enthalpy $\Delta_r H^\circ_{298}$, the formation enthalpy $\Delta_f H^\circ$ −491.620 kJ/mol at 298 K for CF_2Cl_2 [25] was used and the formation enthalpies of the daughter fragments at 0 K were directly cited from the JANAF tables [25]. When the values of the fragments were not available, the data at 298 K from Lias et al. [26] were used. The enthalpies of formation for F_2^+, FCl^+, and Cl_2^+ were estimated indirectly using the IP_a values of F_2 (15.6943 eV) [27], FCl (12.66 ± 0.01 eV) [28], Cl_2 (11.4864 ± 0.0001 eV) [29] and the 0 K $\Delta_f H^\circ$ values of F_2, FCl, and Cl_2 [25]. For CFCl, we used a value of $\Delta_f H^\circ$ 14 kJ/mol taken from ref. [30]. To estimate the enthalpies of the ion-pair dissociations including the excited-state fragments, the energies of the excited-state fragments CF_2, CF_2^+, CFCl, CCl_2, and CCl^+ were taken from the standard sources [31] and ref. [32], while the 0 K $\Delta_f H^\circ$ values of the excited-state fragments, $Cl^-(^3P)$, $CF^+(^3\Sigma)$, $CF_2Cl^+(^3A")$, $CFCl^+(^4A")$, and $FCl(^3\Sigma)$, were calculated at the G3MP2 level [33] by GAUSSIAN 03 program [34].

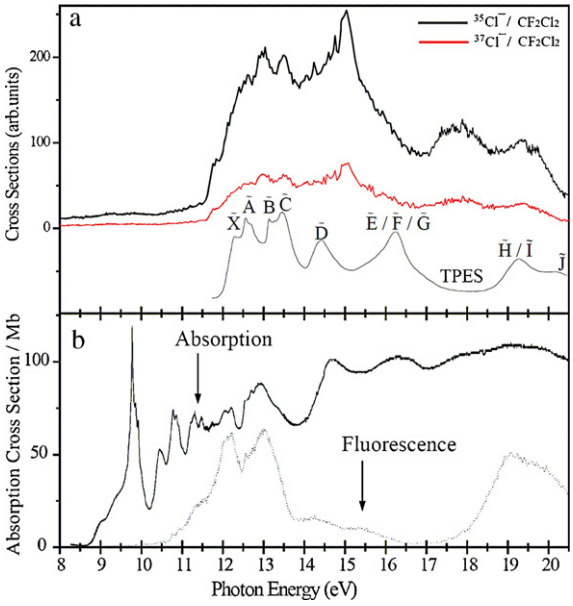

Fig. 1. (a) The anion yield spectra for $^{35}Cl^-$ and $^{37}Cl^-$ and the threshold photoelectron spectrum (TPES) of CF_2Cl_2 which is reproduced from ref. 18 (with the copyright permission from AIP) for comparison. (b) VUV photoabsorption (upper) and fluorescence excitation (below) spectra of CF_2Cl_2 are reproduced from ref. 16 (with the copyright permission from AIP) for comparison.

3. Results and discussion

The negative ion mass spectra for CF_2Cl_2 recorded in this work only show the presence of three anions: F^-, $^{35}Cl^-$, and $^{37}Cl^-$. No other anions were observed in the experiment, which may be due to their much lower yield efficiencies. The IPAES (8.00–20.50 eV) of $^{35}Cl^-$ and $^{37}Cl^-$ are depicted in Fig. 1, meanwhile the photoabsorption and fluorescence excitation spectra [16] and the threshold photoelectron spectrum (TPES) [18] have been reproduced for comparison. Since no distinct isotopic effect is found for the IPAES of $^{35}Cl^-$ and $^{37}Cl^-$, only the spectrum of $^{35}Cl^-$ is analyzed in the following text. In the low energy range of 8.00–11.60 eV, the electron excitation assignments of the valence-to- valence and valence-to-Rydberg states are made for the IPAES of Cl^- in Fig. 2. Correspondingly, the energies for the electron transitions are listed in Table 1. For the photon energies higher than the lowest vertical ionization potential (IP_v), 12.26 eV for $\tilde{X}^2$ B_2 ionization state [19], the energetically accessible multi-body fragmentation channels to produce Cl^- are assigned, as shown in Fig. 3 and listed in Table 2. In Figs. 3 and 4, the multi-body fragmentation channels are tentatively assigned for the IPAES of Cl^- and F^- in the photon energy of 17.30–20.50 eV. The accessible multi-body fragmentation channels to produce F^- in this energy range are tabulated in Table 3.

3.1. Formation of Cl^-

As shown in Fig. 1a, the IPAES of $^{35}Cl^-$ and $^{37}Cl^-$ show the identical spectral features, except that the spectral intensity ratio of $^{35}Cl^-$

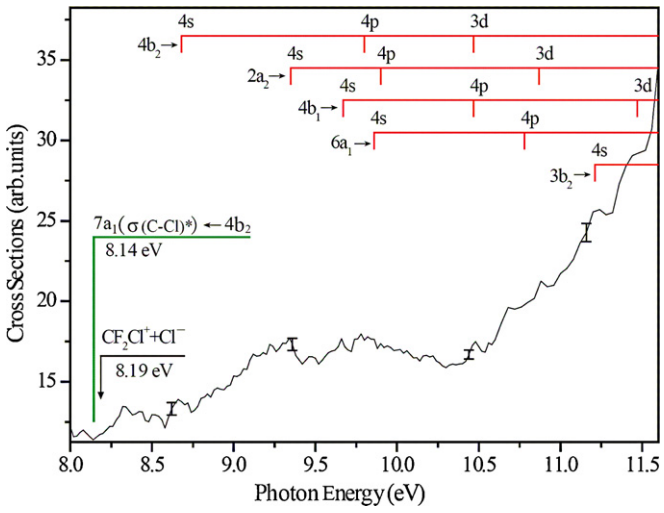

Fig. 2. The Cl^- production efficiency curve in the energy range of 8.00–11.60 eV. Statistical errors are shown at the selected energies. Five sets of valence to Rydberg state transitions, one valence to valence transition, and the lowest threshold for the ion-pair dissociation are assigned.

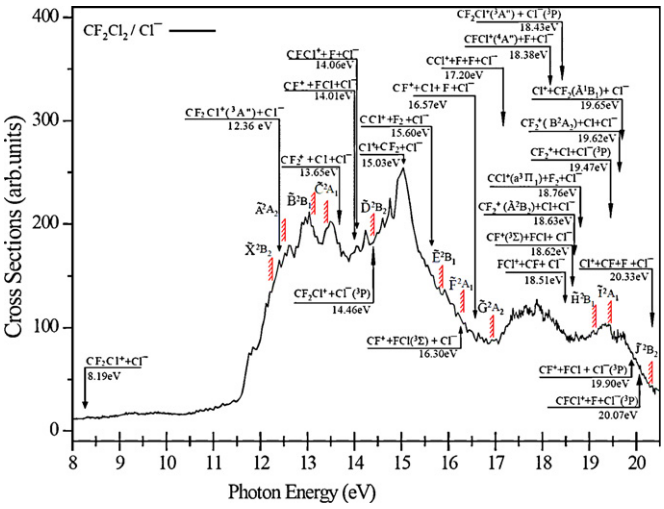

Fig. 3. Multi-body fragmentation channels and the IP_v values for the outer valence MOs are assigned in the spectrum of Cl^-.

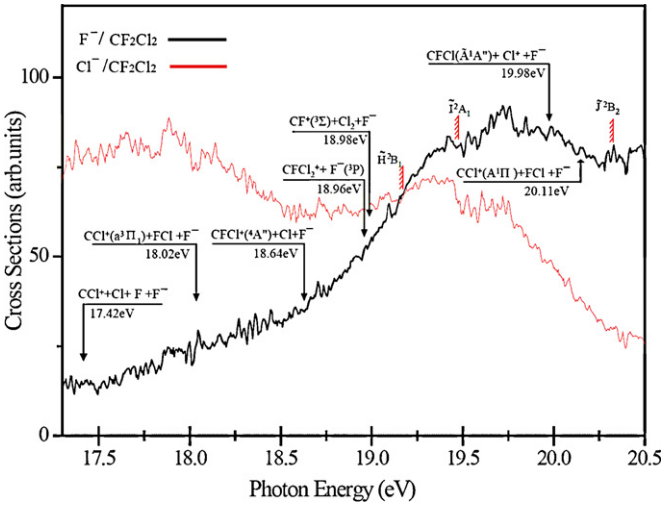

Fig. 4. Competition between Cl^- and F^- productions in the higher energy range. The multi-body fragmentation channels to produce F^- are assigned.

Table 1
Rydberg assignments of the peak features in the Cl^- efficiency curve.

Peak position (eV)	Assignment	Δ
8.265[b] 8.14,[d] 8.11[e]	$7a_1(\sigma(C–Cl)^*) \leftarrow 4b_2$	
8.68[a] 8.940[b] 8.926[d]	$4s \leftarrow 4b_2$	2.05[a] 1.98[b] 1.98[d]
9.35[a] 9.380,[b] 9.360[d]	$4s \leftarrow 2a_2$	1.93[a] 1.92[b] 1.93[d]
9.67[a] 9.612[b] 9.641[d]	$4s \leftarrow 4b_1$	2.01[a] 2.03[b] 2.02[d]
9.802[b] 9.801[d]	$4p \leftarrow 4b_2$	1.65[b] 1.65[d]
9.857[b] 9.935[d]	$4s \leftarrow 6a_1$	2.05[b] 2.03[d]
9.904[b] 9.871[d]	$4p \leftarrow 2a_2$	1.72[b] 1.94[d]
10.473[b] 10.472[d]	$3d \leftarrow 4b_2$	0.24[b] 0.24[d]
	$4p \leftarrow 4b_1$	1.73[b] 1.73[d]
10.783[b] 10.781[d]	$4p \leftarrow 6a_1$	1.74[b] 1.74[d]
10.876[b]	$3d \leftarrow 2a_2$	0.13[b]
11.22[a] 11.323[b]	$4s \leftarrow 3b_2$	1.92[a] 1.88[b]
11.480[b]	$3d \leftarrow 4b_1$	0.11[b]
11.75[c]	$3d \leftarrow 6a_1$	0.17[c]
	$3s \leftarrow 3b_1$	1.19[c]
12.07[c]	$4p \leftarrow 3b_2$	1.56[c]
12.22[c]	$4p \leftarrow 3b_2$	1.48[c]
12.96[c]	$5s \leftarrow 3b_2$	1.88[c]
14.72[c]	$4p \leftarrow 3b_1$	0.60[c]
	$4s \leftarrow 5a_1$	1.07[c]
	$4p \leftarrow 1a_2$	1.50[c]
16.5[c]	$nl \leftarrow 2b_1$	

[a] Obtained in this work.
[b] Cited from Ref. [15].
[c] Cited from Ref. [16].
[d] Cited from Ref. [17].
[e] Cited from Ref. [14].

and $^{37}Cl^-$ is about 3: 1 (as their natural isotope abundance ratio). In comparison with the TPES [18], the IPAES also exhibit several peaks in the energy of 12.00–14.00 eV, approximately corresponding to the first four ionization states, $\widetilde{X}$, $\widetilde{A}$, $\widetilde{B}$, and $\widetilde{C}$. However, the peak of $\widetilde{D}$ state in the TPES corresponds in energy to the big shoulder around 14.5 eV, while a distinct strong speak in the IPAES is observed at 15.03 eV. In the similar scenario, the seriously overlapped band, $\widetilde{E}/\widetilde{F}/\widetilde{G}$, in the TPES, corresponds in energy to the shoulder around 16.0 eV in the IPAES. Such similar spectral features imply that some ion-pair dissociation channels to produce Cl^- may resonantly couple the valence-to-high Rydberg state transitions converging to the respective ionization states. However, in contrast to the TPES, one additional broad band around 17.5 eV is observed in the IPAES. As shown in Fig. 1b, the photoabsorption and fluorescence excitation spectra [16] are significantly different from the IPAES, in particular, below 11 eV there are several strong peaks in the photoabsorption spectrum [16] while the production curve of Cl^- is much low and flat. When we zoom into the IPAES, as shown in Fig. 2, there are several bumped bands. The details will be discussed in the following text.

Before assignments to the IPAES recorded in this work, the arguments on the ionization states should be recalled. As suggested by Shan et al. [21], a new and unambiguous order of molecular orbitals (MOs) is,

$$(\text{core})^{26}\underbrace{(1a_1)^2(1b_2)^2(2a_1)^2(1b_1)^2}_{\text{inner-valence}}$$

$$\underbrace{(3a_1)^2(2b_2)^2(4a_1)^2(2b_1)^2(1a_2)^2(5a_1)^2(3b_1)^2(3b_2)^2(6a_1)^2(4b_1)^2(2a_2)^2(4b_2)^2}_{\text{outer-valence}}$$

Thus we will use the above MO sequence in the present assignments, moreover, the corrections to the previous wrong assignments will be declared when necessary. In the photoabsorption spectra [14–17] and the IPAES [4,5,8,23,24], the Rydberg-serial structures are frequently observed and each peak indicates an elec-

Table 2
Energetics of the ion-pair dissociations to produce Cl^- and the IP_v values of CF_2Cl_2.

Neutral/parent ion	Ion-pair dissociation channel	Dissociation energy (eV)	IP_v (eV)
$CF_2Cl_2^+\tilde{J}^2B_2$			20.40[c] 20.30[d]
	$Cl^+ + CF + F + Cl^-$	20.33[a]	
	$CFCl^+ + F + Cl^-$ (^3P)	20.07[b]	
	$CF^+ + FCl + Cl^-$ (^3P)	19.90[b]	
	$Cl^+ + CF_2(\tilde{A}^1B_1) + Cl^-$	19.65[a]	
	$CF_2^+(\tilde{B}^2A_2) + Cl + Cl^-$	19.62[a]	
	$CF_2^+ + Cl + Cl^-$(^3P)	19.47[b]	
$CF_2Cl_2^+\tilde{I}^2A_1$			19.3[c] 19.29[d]
$CF_2Cl_2^+\tilde{H}^2B_1$			19.3[c] 19.29[d]
	$CCl^+(a^3\Pi_1) + F_2 + Cl^-$	18.76 [a]	
	$CF_2^+(\tilde{A}^2B_2) + Cl + Cl^-$	18.63[a]	
	$CF^+(^3\Sigma) + FCl + Cl^-$	18.62[b]	
	$FCl^+ + CF + Cl^-$	18.51[a]	
	$CF_2Cl^+(^3A'') + Cl^-(^3P)$	18.43[b]	
	$CFCl^+(^4A'') + F + Cl^-$	18.38[b]	
	$CCl^+ + F + F + Cl^-$	17.20[a]	
$CF_2Cl_2^+\tilde{G}^2A_2$			16.90[c] 16.24[d]
	$CF^+ + Cl + F + Cl^-$	16.57[a] 16.42[b]	
	$CF^+ + FCl(^3\Sigma) + Cl^-$	16.30[b] 16.23[e]	
$CF_2Cl_2^+\tilde{F}^2A_1$			16.30[c] 16.24[d]
$CF_2Cl_2^+\tilde{E}^2B_1$			15.90[c] 16.24[d]
	$CCl^+ + F_2 + Cl^-$	15.60[a]	
	$Cl^+ + CF_2 + Cl^-$	15.03[a]	
	$CF_2Cl^+ + Cl^-(^3P)$	14.46[b]	
$CF_2Cl_2^+\tilde{D}^2B_2$			14.36[c] 14.41[d]
	$CFCl^+ + F + Cl^-$	14.06[a] 14.00[b]	
	$CF^+ + FCl + Cl^-$	14.01[a] 13.83[b]	
	$CF_2^+ + Cl + Cl^-$	13.65 [a]	
$CF_2Cl_2^+\tilde{C}^2A_1$			13.45[c] 13.45[d]
$CF_2Cl_2^+\tilde{B}^2B_1$			13.11[c] 13.14[d]
$CF_2Cl_2^+\tilde{A}^2A_2$			12.53[c] 12.55[d]
	$CF_2Cl^+(^3A") + Cl^-$	12.36[b]	
$CF_2Cl_2^+\tilde{X}^2B_2$			12.26[c] 12.28[d]
	$CF_2Cl^+ + Cl^-$	8.19[a] 8.39[b]	
$CF_2Cl_2\tilde{X}^1A_1$			0.00

[a] Calculated in this work using the standard thermochemistry data.
[b] At the G3MP2 level calculated in this work.
[c] Cited from Ref. [19].
[d] Cited from Ref. [18].
[e] Estimated with the experimental data from Ref. [22].

Table 3
Energetics of Ion-pair dissociations to produce F^-.

Ion-pair dissociation channel	Dissociation energy (eV)
$Cl^+ + CF + Cl + F^-$	20.56[a]
$CCl^+(A^1\Pi) + FCl + F^-$	20.11[a]
$Cl^+ + CFCl(\tilde{A}^1A") + F^-$	19.98[a]
$CF^+(^3\Sigma) + Cl_2 + F^-$	18.98[b]
$CFCl_2^+ + F^-(^3P)$	18.96[b]
$CFCl^+(^4A") + Cl + F^-$	18.64[b]
$CCl^+(a^3\Pi_1) + FCl + F^-$	18.02[a]
$CCl^+ + Cl + F + F^-$	17.42[a]

[a] Calculated in this work using the standard thermochemistry data.
[b] At the G3MP2 level calculated in this work.

tron transition from a valence MO to a Rydberg orbital with the energy E_R,

$$E_R = IP_v - \frac{R}{(n-\delta)^2} \quad (2)$$

where R is the Rydberg constant (13.60569 eV), n is the principal quantum number, and δ is the quantum defect resulting from the penetration of the Rydberg orbital into the core. According to the Rydberg-serial assignments proposed by Doucet et al. [14], Ibuki et al. [15], Seccombe et al. [16], and Limão Vieira et al. [17], five sets of valence to Rydberg state transitions, $4b_2$, $2a_2$, $4b_1$, $6a_1$, $3b_2 \rightarrow nl$ ($l = 0, 1, 2$, etc.), are tentatively assigned in Fig. 2. The quantum defects δ for each series are cited from the literatures and adjusted slightly for the best fittings to the small peaks embedded on the diffuse bands in the present IPAES. As listed in Table 1, the derivations of the present fitted δ values are less than 0.06, and the fitted E_R values are also in good agreement with the data reported previously [15,17]. Meanwhile, there are two vibrational progressions observed in the photoabsorption spectra, i.e., $n\nu_9$ (CCl stretching mode) in the energy range of 8.50–9.25 eV [15,17] and $n\nu_4$ (CCl_2 scissor mode) in the energy range of 11.4–11.9 eV [16]. However, these two vibrational progresses do not stand out either in the present IPAES or that reported previously [7]. In the present IPAES, see Fig. 1a, the ladder-like structures embedded on the band shoulder (11.50–11.90 eV) imply that the $n\nu_4$ vibrational excitations are possibly coupling with ion-pair states, but the valence-to-Rydberg state transitions, e.g., $6a_1 \rightarrow 3d$ and $3b_1 \rightarrow 3s$ ($E_R = 11.75$ eV) [16], may also be involved in this energy range. According to the MO characters, two highest occupied MOs, $4b_2$ and $2a_2$, are basically consisted of the atomic lone-pair $3p$ (n_{Cl}) orbitals. In the photoabsorption spectra, a broad and weak band was determined to be centered at 8.11 eV (65400 cm^{-1}) [14], 8.265 eV (150 nm) [15], and 8.14 eV [17], respectively, with the common assignment as the valence-to-valence transition, i.e., $4b_2$ (n_{Cl}) to an anti-bond σ*(C–Cl) orbital. Here in the spectrum (see Fig. 2), a valence-to-valence transition, $4b_2$ (n_{Cl}) → $7a_1$ (σ*(C–Cl)), is tentatively assigned at 8.14 eV, where $7a_1$ is the lowest unoccupied MO having the anti-bond σ*(C–Cl) characteristics. However, it is noted that the threshold to produce Cl^-, $CF_2Cl_2 + h\nu \rightarrow Cl^- + CF_2Cl^+$, is determined to be 8.19 eV with the standard thermochemistry data [25]. This value is in excellent agreement with the present observation, i.e., an onset at 8.20 ± 0.04 eV. On the other hand, it is possible that the intervalence excitation $4b_2$ (n_{Cl}) → $7a_1$ (σ*(C–Cl)) couples the lowest ion-pair dissociation channel $CF_2Cl_2 + h\nu \rightarrow Cl^- + CF_2Cl^+$ because of their extremely close energies.

Besides the valence-to-Rydberg state transitions discussed above, there are more electron transitions occurring at the higher energies. As listed in Table 1, $3b_2 \rightarrow 4p$, $3b_2 \rightarrow 5s$, and $3b_1 \rightarrow 4p$, $5a_1 \rightarrow 4s$, $1a_2 \rightarrow 4p$ transitions can somehow correspond to the small peaks or shoulders at the respective energies in the spectrum in Fig. 3. On the other hand, a lot of fragmentation channels can be accessible at the energies higher than 12 eV. Their energetic thresholds $E_{Threshold}$ estimated with Eq. (1) and calculated at the G3MP2 [33] level are listed in Table 2, and the fragmentation channels and the IP_v positions for the outer-valence MOs are assigned in Fig. 3. In comparison with the thermochemistry results of $E_{Threshold}$, one can find that the G3MP2 results are quite good and the derivations are less than 0.2 eV. In general, with the increase of photon energy, more multi-body fragmentation processes may be involved in the ion-pair dissociations. The position 15.00 eV of the most prominent peak happens to be close to the dissociation threshold, $CF_2Cl_2 + h\nu \rightarrow Cl^- + CF_2 + Cl^+$ ($E_{Threshold} = 15.03$ eV).

At the higher energy end of the Cl^- yield spectrum in Fig. 3, there are many fine structures and about thirteen multi-body fragmentation channels might be responsible for the two broad bands at 17.5 and 19.5 eV. A plenty of structures may be observed in this region, because the Cl^- ion efficiency curve is recorded with a smaller scanning step of 5 meV. Around photon energy 19.3 eV, two ionization states, $\tilde{H}$ and $\tilde{I}$, were assigned in the TPES [18] and the photoelectron spectrum [19]. However, the contrary terms were named as $\tilde{H}^2A_1/\tilde{I}^2B_1$ [16] but $\tilde{H}^2B_1/\tilde{I}^2A_1$ [18] by the same group. According to the recent *ab initio* calculations [35], IP_v ($\tilde{H}^2B_1$: $2b_1^{-1}$) ~ 19.15 eV and IP_v ($\tilde{I}^2A_1$: $4a_1^{-1}$) ~ 19.45 eV, are tentatively assigned in the Cl^- IPAES, and the averaged IP_v for these two ion-

ization states happens to be 19.30 eV which is exactly the same as the experimental IP value for the overlapped band observed in the previous spectra [18,19]. On the basis of the previous suggestion, the valence to Rydberg state transitions, $2b_1 \rightarrow nl$, were converged to IP = 19.3 eV [16]. Therefore, besides the multi-body fragmentation processes involved in the ion-pair dissociations as mentioned above, the coupling between the high Rydberg states and the ion-pair dissociations should be considered. However, there are no other spectroscopic supports for this speculation, we will not discuss more about the valence to Rydberg state transitions in this energy range.

Several dissociation channels including the exited-state fragments are predicted at the G3MP2 level in this work. In Table 2, the excited-state fragments, for instance, FCl ($^3\Sigma$), CF_2Cl^+ ($^3A''$), and CCl^+ ($a^3\Pi$), may be produced in the high-spin (triplet-state) dissociation channels that are coupled with some photoexcited singlet-state potential surface by passing through the conical cones. Until now, the life-times of these metastable-state ions are unknown, which strongly influences the possibility to detect them using the conventional quadruple mass filter or the TOF mass spectrometer. Near the photon energy of 19 eV, six ion-pair channels to $CClF^+(^4A'') + F(^2P) + Cl^-(^1S)$ (18.38 eV), $CF_2Cl^+(^3A'') + Cl^-(^3P)$ (18.51 eV), $FCl^+ + CF + Cl^-$ (18.43 eV), $CF^+(^3\Sigma) + FCl + Cl^-$ (18.62 eV), $F_2{}^+(\tilde{A}^2B_2) + Cl + Cl^-$ (18.63 eV), and $CCl^+(a^3\Pi_1) + F_2 + Cl^-$ (18.76 eV) can be accessed. In these channels (excluding the channel to $FCl^+ + CF + Cl^-$), at least one fragment is at the metastable state. For the threshold energies higher than 19 eV, the metastable $Cl^-(^3P)$ can be produced frequently in three ion-pair channels, while the ground-state Cl^- (^1S) can be produced in another three channels as well. In this energy range, the neutral fragmentation, $Cl_2(D'2^3\Pi_g) + C + F_2$ (19.53 eV), can also be accessed [16]. As a cascade process, the Cl^- ion may also be produced through the dissociation of the ion-pair state $Cl_2(D'2^3\Pi_g)$ species, induced by the strong pulsed field (16,500 V/m applied to the reaction area, see discussion in Ref. [24]) used in the present TOF mass spectrometer.

3.2. Formation of F^-

Since the large aperture (diameter: 10 mm) ion lenses are employed in the present TOF mass spectrometer and the strong pulsed field is applied to the repeller in the experiments, we assume that the collection efficiency is almost unity for the different ions and even at the high photon energies where the ionic fragment may have a kinetic energy of 1–2 eV. In this work, a novel competition of production efficiency is observed between Cl^- and F^-. As shown in Fig. 4, the F^- ion efficiency cure is depicted in the energy range 17.30–20.50 eV. It has been pointed out that the threshold to produce F^- could be as low as 12.07 eV [22]. In this work, the F^- ion has been found in the mass spectra below 17.30 eV, but its ion intensity is too low to be analyzed. In Fig. 4, the Cl^- production is much stronger than the F^- yield at the lower energies, while their efficiency curves cross at 19.15 eV which happens to be IP_v of $\tilde{H}^2B_1$. According to the MO properties, i.e., $2b_1$ (C-F bonding) and its next MO $4a_1$ (C-F bonding) [35], the transitions, $2b_1/4a_1 \rightarrow np_F/ns_F$, may also play roles in the production preference of F^- at the higher photon energies. When carefully examining the fine structures of these two curves, one can find that they show almost identical structures, implying that Cl^- and F^- may be produced through the common excited intermediate state in this energy range. However, the thermochemistry of the ion-pair dissociations to produce F^- is different from that for Cl^-. The multi-body fragmentation channels to produce F^- are tentatively assigned in Fig. 4 and listed in Table 3.

There are a lot of arguments about the sources of the smaller cationic fragments such as $CFCl^+$ and CF^+ at the photon energies higher than ca. 16 eV [18,22,36]. For example, the different AE values for $CClF^+$ determined to be were 15.2 ± 0.3 eV and 17.50 ± 0.05 eV, and they were attributed to $CFCl^+ + Cl + F^-$ and $CFCl^+ + F + Cl^-$, respectively [22]. However, the thermochemical thresholds predicted in this work for $CFCl^+ + Cl + F^-$ and $CFCl^+ + F + Cl^-$, are 14.28 eV (see Table 3) and 14.06 eV (see Table 2), respectively. Those much higher AEs [22] may be due to some dynamic mechanisms in the ion-pair dissociations, e.g., to overcome an inherent dissociative barrier.

4. Conclusion

Negative ions $^{35}Cl^-$, $^{37}Cl^-$, and F^- are observed in the VUV photodissociations of CF_2Cl_2 using synchrotron radiation and their ion production efficiency curves are recorded in the wide photon energy range of 8.00–20.50 eV. The fragmentation enthalpies are estimated on the basis of the high-level G3MP2 calculations performed in this work and with the thermochemistry data available in the literatures. It is advantageous to determine the ion pairs below the molecular IP_a value from an experiment point of view if only energetically accessible. Since there are no background signals, the anions can be detected with the confidence that they must be produced through the ion-pair dissociation. Based on this condition, the Cl^- production curve is successfully recorded below the first ionization threshold, and assigned with the valence-to-Rydberg state transitions. Moreover, the energetic threshold for $CF_2Cl_2 + h\nu \rightarrow Cl^- + CF_2Cl^+$ is determined to be 8.20 ± 0.04 eV, in excellent agreement with the theoretical value 8.19 eV estimated with the standard thermochemistry data. A lot of multi-body fragmentation processes are predicted with the present thermochemistry calculations, and used in the spectral assignments. For the first time, F^- anionic fragment is observed in the energy range of 17.30–20.50 eV, more interestingly, we find a novel competition between the ion-pair photodissociations to Cl^- and F^-.

Acknowledgements

This work is supported by NSFC (Grant Nos. 10775130 and 10979048), MOST (Grant Nos. 2007CB815204 and 2011CB921401), USTC-NSRL association funding, and the Fundamental Research Funds for the Central Universities (Grant No. WK2340000012).

References

[1] J. Berkowitz, in: U. Becker, D.A. Shirley (Eds.), VUV and Soft-Ray Photoionization, Plenum, New York, 1996, p. 263.
[2] A.G. Suits, J.W. Hepburn, Annu. Rev. Phys. Chem. 57 (2006) 431.
[3] S.W. Scully, J.R.A. Mackie, R. Browning, K.F. Dunn, C.J. Latimer, Phys. Rev. A 70 (2004) 042707.
[4] K. Mistuke, H. Hottori, H. Yoshita, J. Chem. Phys. 99 (1993) 6642.
[5] S. Suzuki, K. Mistuke, T. Imamura, I. Koyano, J. Chem. Phys. 96 (1992) 7500.
[6] M.J. Simpson, R.P. Tuckett, K.F. Dunn, C.A. Hunniford, C.J. Latimer, J. Chem. Phys. 130 (2009) 194302.
[7] D.A. Shaw, D.M.P. Holland, I.C. Walker, J. Phys. B 39 (2006) 3549.
[8] S.X. Tian, Y.F. Xu, Y.F. Wang, Q. Feng, L.L. Chen, J.D. Sun, F.Y. Liu, X.B. Shan, L.S. Sheng, Chem. Phys. Lett. 496 (2010) 254.
[9] H. Hotop, M.W. Ruf, I.I. Fabrikant, Phys. Script T110 (2004) 22.
[10] W.A. Chupka, P.M. Dehmer, W.T. Jivery, J. Chem. Phys. 63 (1975) 3929.
[11] P.M. Dehmer, W.A. Chupka, J. Chem. Phys. 62 (1975) 4525.
[12] M.J. Molina, F.S. Rowland, Rev. Geophys. Space 13 (1975) 1.
[13] C.R. Zobel, A.B.F. Duncan, J. Am. Chem. Soc. 77 (1955) 2611.
[14] J. Doucet, P. Sauvageau, C. Sandorfy, J. Chem. Phys. 58 (1973) 3708.
[15] T. Ibuki, A. Hiraya, K. Shobatake, J. Chem. Phys. 90 (1989) 6290.
[16] D.P. Seccombe, R.Y.L. Chim, R.P. Tuckett, H.W. Jochims, H. Baumgartel, J. Chem. Phys. 114 (2001) 4058.
[17] P. Limão Vieira, S. Eden, P.A. Kendall, N.J. Mason, S.V. Hoffmann, Chem. Phys. Lett. 364 (2002) 535.
[18] D.P. Seccombe, R.P. Tuckett, B.O. Fisher, J. Chem. Phys. 114 (2001) 4074.
[19] T. Cvitaš, H. Güsten, L. Klasinc, J. Chem. Phys. 67 (1977) 2687.
[20] T. Pradeep, D.A. Shirley, J. Electron Spectrosc. Relat. Phenomen. 66 (1993) 125.
[21] X. Shan, X.J. Chen, L.X. Zhou, Z.J. Li, T. Liu, X.X. Xue, K.Z. Xu, J. Chem. Phys. 125 (2006) 154307.
[22] H. Schenk, H. Oertel, H. Baumgärtel, Ber. Bunsenges. Phys. Chem. 83 (1979) 683.

[23] Q. Feng, S.X. Tian, Y.J. Zhao, F.Y. Liu, X.B. Shan, L.S. Sheng, Chin. Phys. Lett. 26 (2009) 053402.
[24] L.L. Chen, Y.F. Xu, Q. Feng, S.X. Tian, F.Y. Liu, X.B. Shan, L.S. Sheng, J. Phys. Chem. A (2011), A 115 4248.
[25] M.W. Chase, J. Phys. Chem. Ref. Data Monogr. 9 (1998).
[26] S.G. Lias, J.E. Bartmess, J.F. Liebman, J.L. Holmes, R.D. Lerin, W.G. Mallard, J. Phys. Chem. Ref. Data Suppl. 17 (1988) 1.
[27] J. Yang, Y. Hao, J. Li, C. Zhou, Y. Mo, J. Chem. Phys. 122 (2005) 134308.
[28] R.L. DeKock, B.R. Higginson, D.R. Lloyd, A. Breeze, D.W.J. Cruickshank, D.R. Armstrong, Mol. Phys. 24 (1972) 1059.
[29] J. Yang, Y. Hao, J. Yang, C. Zhou, Y. Mo, J. Chem. Phys. 127 (2007) 104307.
[30] C.F. Rodriquez, A.C. Hopkinson, J. Phys. Chem. 97 (1993) 849.
[31] M.E. Jacox, J. Phys. Chem. Ref. Data Monogr. 3 (1994).
[32] M. Tsuji, T. Mizuguchi, K. Shinohara, Y. Nishimura, Can. J. Phys. 61 (1983) 838.
[33] L.A. Curtiss, P.C. Redfern, K. Raghavachari, V. Rassolov, J.A. Pople, J. Chem. Phys. 110 (1999) 4703.
[34] M. J. Frisch, G.W. Trucks, H.B. Schlegel, G.E. Scuseria, M.A. Robb, J.R. Cheeseman, J.A. Montgomery, Jr., T. Vreven, K.N. Kudin, J.C. Burant, J.M. Millam, S.S. Iyengar, J. Tomasi, V. Barone, B. Mennucci, M. Cossi, G. Scalmani, N. Rega, G.A. Petersson, H. Nakatsuji, M. Hada, M. Ehara, K. Toyota, R. Fukuda, J. Hasegawa, M. Ishida, T. Nakajima, Y. Honda, O. Kitao, H. Nakai, M. Klene, X. Li, J.E. Knox, H.P. Hratchian, J.B. Cross, C. Adamo, J. Jaramillo, R. Gomperts, R.E. Stratmann, O. Yazyev, A.J. Austin, R. Cammi, C. Pomelli, J.W. Ochterski, P.Y. Ayala, K. Morokuma, G.A. Voth, P. Salvador, J.J. Dannenberg, V.G. Zakrzewski, S. Dapprich, A.D. Daniels, M.C. Strain, O. Farkas, D.K. Malick, A.D. Rabuck, K. Raghavachari, J.B. Foresman, J.V. Ortiz, Q. Cui, A.G. Baboul, S. Clifford, J. Cioslowski, B.B. Stefanov, G. Liu, A. Liashenko, P. Piskorz, I. Komaromi, R.L. Martin, D.J. Fox, T. Keith, M.A. Al-Laham, C.Y. Peng, A. Nanayakkara, M. Challacombe, P.M. W. Gill, B. Johnson, W. Chen, M.W. Wong, C. Gonzalez, and J. A. Pople, Gaussian, Inc., Pittsburgh PA, (2003).
[35] B. Sierra, R. Martínez, F. Castaño, J. Phys. B: At. Mol. Opt. Phys. 37 (2004) 295.
[36] H.W. Jochims, W. Lohr, H. Baumgärtel, Ber. Bunsenges. Phys. Chem. 80 (1976) 130.